Shear-Induced Instability of the Lamellar Phase of a Block Copolymer

Hiroya Kodama* and Masao Doi

Department of Applied Physics, Faculty of Engineering, Nagoya University, Nagoya 464-01, Japan

Received August 21, 1995; Revised Manuscript Received January 3, 1996[⊗]

ABSTRACT: We conducted a computer simulation for the structural changes of randomly oriented lamellae of block copolymers under steady shear flow and observed two types of structural changes: one is breakup and recombination of lamellae, and the other is undulation of lamellae. To interpret these phenomena, we analyzed the stability of a lamellar structure when its periodicity is changed. We found that there are three types of instability: (1) The Eckhaus type, which causes nonuniform lamellar spacing, (2) an undulational type, which causes undulated lamellae, and (3) a melting type, which entirely destroys the lamellar structure. Using the complex amplitude equation for the modulated lamellae, we obtain the phase diagram for these instabilities.

1. Introduction

One of the distinctive features of block copolymers is that, in the ordered equilibrium phase, they exhibit mesoscale periodic structures consisting of lamellae, cylinders, or spheres. It has been shown that flow fields affect these mesoscale structures, giving rise to global orientation[1,2] of lamellae or cylinders. In particular, many experimental works[3−10] have been reported recently studying the direction of final (or steady) alignment of lamellae of block copolymers under shear, varying the shearing conditions and the temperature. The alignment achieved by shear was first found to be "parallel", i.e., lamellar normals are parallel to the shear gradient direction,[2,4] but recently, other alignments such as "perpendicular" and "transverse" alignments in which the lamellar normals are parallel to the vortex direction[3,5,7−9] and to the velocity direction,[6,10] respectively, have been observed. In spite of these considerable experimental works, a clear answer to the mechanisms for flow-induced lamellar alignment was not obtained.

On the theoretical side, Amundson and Helfand[11] first studied the stability of the lamellar structure in block copolymers under deformation and showed that the lamellar phase can be transformed into a disordered state if the deformation is large. They also calculated the elastic deformation constants of lamellar block copolymers. Further analysis of the problem was done by Wang,[12] who showed that the stretching deformation causes lamellar undulation giving an anomalous elastic response. Williams and MacKintosh[13] studied the behavior of lamellae alternatively sheared along their planes and showed that it can induce lamellar undulation at high frequency. All these theories are quasistatic, and only the free energy change is analyzed. On the other hand, theories based on kinetic equations have been proposed by Fredrickson[14] and by Goulian and Milner,[15] who analyzed the steady-state orientation of lamellar phases under the steady shear flow.

In this paper, we consider the problem of how a randomly oriented lamellar morphology changes its structure toward the perfectly oriented lamellar morphology when a shear is applied. To answer this question, we performed computer simulation based on the Ohta−Kawasaki model[16] for block copolymers using the cell dynamical scheme proposed by Oono et al.[17−19] The result indicates that there are two typical structural changes of lamellae: one is the breakup and recombination of lamellae and the other is the undulation of lamellae. The former of these structural changes occurs in the region where lamellae are compressed, and the latter occurs in the expanded region. Therefore these structural changes can be attributed to an effect of shear causing compression or expansion of each lamellar grain (see Figure 1).

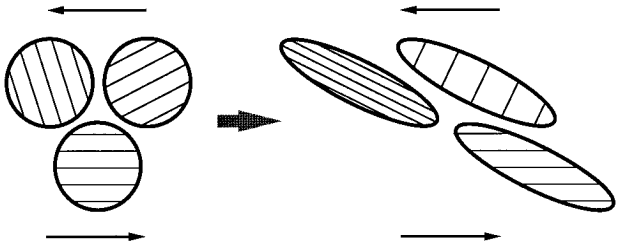

Figure 1. Schematics of the compression or expansion effect for lamellar grains due to shear deformation.

To confirm this, we studied both numerically and analytically whether the lamellar structure remains stable or not when its periodicity is changed. This is the same problem as that studied in the earlier works,[11,12] but the expression of the free energy is different and the method of the analysis is more general in our approach. For the present problem, we found that there are three types of instability: (1) The Eckhaus type, (2) an undulational type, and (3) a melting type. The Eckhaus instability signifies a compression/dilatation instability with a long wavelength (nonuniform lamellar spacing) and has been observed in convection roll systems such as Rayleigh−Bénard convections.[20] From the analysis, we construct the phase diagram for the instabilities.

2. Basic Equation

We consider a block copolymer consisting of two homopolymer blocks A and B, each having the degree of polymerization N_A and N_B, respectively. The total degree of polymerization is $N = N_A + N_B$ and the ratio of the A block is $f = N_A/N$. In the present study, we focus our attention on the symmetric case, i.e., $f = 0.5$. We use the model proposed by Ohta and Kawasaki[16] for the block copolymer mesophase. This model has

[⊗] Abstract published in *Advance ACS Abstracts,* March 1, 1996.

0024-9297/96/2229-2652$12.00/0

Figure 2. Density profile of the randomly oriented lamellar structure obtained by the simulation with $\dot{\gamma} = 0$ iterated for 10^5 steps.

been used in the investigation of the rheological behavior of the cylindrical hexagonal phases under oscillatory shear flow.[21]

In the Ohta−Kawasaki model, the free energy of the block copolymers is described as a functional of the local segment density of A, B $\rho_A(\mathbf{r})$, $\rho_B(\mathbf{r})$ at point $\mathbf{r}$. We assume that the system is incompressible; i.e., $\rho_A(\mathbf{r}) + \rho_B(\mathbf{r}) \equiv \rho_0$ is constant. The order parameter $\psi(\mathbf{r})$ is defined as the composition difference between the A and B components:

$$\psi(\mathbf{r}) = \frac{\rho_A(\mathbf{r}) - \rho_B(\mathbf{r})}{2\rho_0} \tag{2.1}$$

Within the mean-field approximation, the free energy functional is represented as a sum of two parts,

$$\frac{\hat{H}\{\psi\}}{\rho_0 k_B T} = H_S\{\psi\} + H_L\{\psi\} \tag{2.2}$$

The term $H_S\{\psi\}$ stands for a short-range part,

$$H_S\{\psi\} = \int d\mathbf{r} \left\{ W(\psi) + \frac{1}{2} D(\nabla\psi)^2 \right\} \tag{2.3}$$

where $W(\psi)$ stands for the mixing free energy of the homogeneous blends of disconnected A−B homopolymers and the term $D(\nabla\psi)^2$ represents the free energy cost due to the spatial variation of ψ. The other term $H_L\{\psi\}$ represents a long-range part,

$$H_L\{\psi\} = \frac{1}{2}\alpha \int d\mathbf{r}\, d\mathbf{r}'\, G(\mathbf{r}-\mathbf{r}')(\psi(\mathbf{r})\psi(\mathbf{r}') - \bar{\psi}^2) \tag{2.4}$$

where $\bar{\psi} \equiv 2f - 1$ and the function $G(\mathbf{r})$ is the principal solution of $\nabla^2 G(\mathbf{r}) = -\delta(\mathbf{r})$. The functional form of $W(\psi)$ is rather arbitrary provided $W(\psi)$ has a double minimum. Ohta and Kawasaki assumed a simple polynomial function of $W(\psi)$,

$$W(\psi) = \frac{1}{2} a\psi^2 + \frac{1}{4} g\psi^4 \tag{2.5}$$

with $a < 0$. In our computer simulation, we choose a slightly different expression:

$$W(\psi) = -A \ln(\cosh \psi) + \frac{1}{2}\psi^2 \tag{2.6}$$

since it has been reported[18] that this form of $W(\psi)$ gives better numerical stability. The two expressions can be related to each other through the behavior of $W(\psi)$ for small ψ. Since

$$-A \ln(\cosh \psi) + \frac{1}{2}\psi^2 = \frac{1}{2}(1 - A)\psi^2 + \frac{1}{12} A\psi^4 + \ldots \tag{2.7}$$

we have

$$a = 1 - A, \qquad g = \frac{1}{3} A \tag{2.8}$$

These parameters can be related to molecular characteristics. According to Ohta and Kawasaki,[16] a, D, and α are given in terms of the degree of polymerization N, the segment length b, and the Flory−Huggins parameter χ as

$$a = -\frac{1}{N}(2\chi N - 7.2), \qquad D = \frac{b^2}{3}, \qquad \alpha = \frac{144}{N^2 b^2} \tag{2.9}$$

for $f = 0.5$.

The time evolution of $\psi(\mathbf{r})$ under a given flow field $\mathbf{v}$ is given by the TDGL-type equation with a convective term,

$$\frac{\partial\psi}{\partial t} + \nabla\cdot(\mathbf{v}\psi) = M\nabla^2 \frac{\delta H\{\psi\}}{\partial\psi} \tag{2.10}$$

where M is a transport coefficient. We assume that the flow is a simple shear flow with constant shear rate $\dot{\gamma}$; $v_x = \dot{\gamma} y$, $v_y = v_z = 0$. Thus the time evolution equation employed here becomes

$$\frac{\partial\psi}{\partial t} = -\dot{\gamma} y \frac{\partial\psi}{\partial x} + M\nabla^2\{-D\nabla^2\psi + F(\psi)\} - M\alpha\psi \tag{2.11}$$

where $F(\psi) = dW(\psi)/d\psi$. This equation can be used both to construct an equilibrium lamellar phase (solving it for $\dot{\gamma} = 0$) and to study how the domains are deformed under shear (solving it for a certain value of $\dot{\gamma}$).

3. Computer Simulation

3.1. Simulation Method. In this work, we restricted ourselves to a two-dimensional system. We used the cell dynamical method proposed by Oono et al.[17−19] to solve the time evolution equation (2.11). In this method, the space coordinate is given by the lattice point $\mathbf{n} = (n_x, n_y)$ in an $L \times L$ square lattice of cell size a_0. The discrete version of the Laplacian of an arbitrary function $X(\mathbf{n})$ is given by

$$\nabla^2 X(\mathbf{n}) = \frac{1}{a_0^2}(\langle\langle X(\mathbf{n})\rangle\rangle - X(\mathbf{n})) \tag{3.1}$$

where $\langle\langle X(\mathbf{n})\rangle\rangle$ stands for the following summation of $X(\mathbf{n})$ for the nearest neighbor (n.n.) cells and the next nearest neighbor (n.n.n.) cells;

$$\langle\langle X(\mathbf{n})\rangle\rangle = \frac{1}{6}\sum_{\mathbf{n}=\text{n.n.}} X(\mathbf{n}) + \frac{1}{12}\sum_{\mathbf{n}=\text{n.n.n.}} X(\mathbf{n}) \tag{3.2}$$

Using a_0 and $\tau_0 = a_0^2/M$ as the unit of length and the time scale, we rewrite eq 2.11 in a dimensionless form:

$$\frac{\partial\psi}{\partial t} = -\tilde{\gamma} y \frac{\partial\psi}{\partial x} + \nabla^2\{-\tilde{D}\nabla^2\psi + F(\psi)\} - \tilde{\alpha}\psi \tag{3.3}$$

where $\tilde{\gamma} = \dot{\gamma} a_0^2/M$, $\tilde{D} = D/a_0^2$, and $\tilde{\alpha} = \alpha a_0^2$. Then we can write the cell dynamics equation corresponding to eq 2.11 as a difference equation,

$$\psi(\mathbf{n},t+1) = \psi(\mathbf{n},t) - \frac{1}{2}\tilde{\gamma} n_y[\psi(n_x+1,n_y,t) - \psi(n_x-1,n_y,t)] + \langle\langle I(\mathbf{n},t)\rangle\rangle - I(\mathbf{n},t) - \tilde{\alpha}\psi(\mathbf{n},t) \tag{3.4}$$

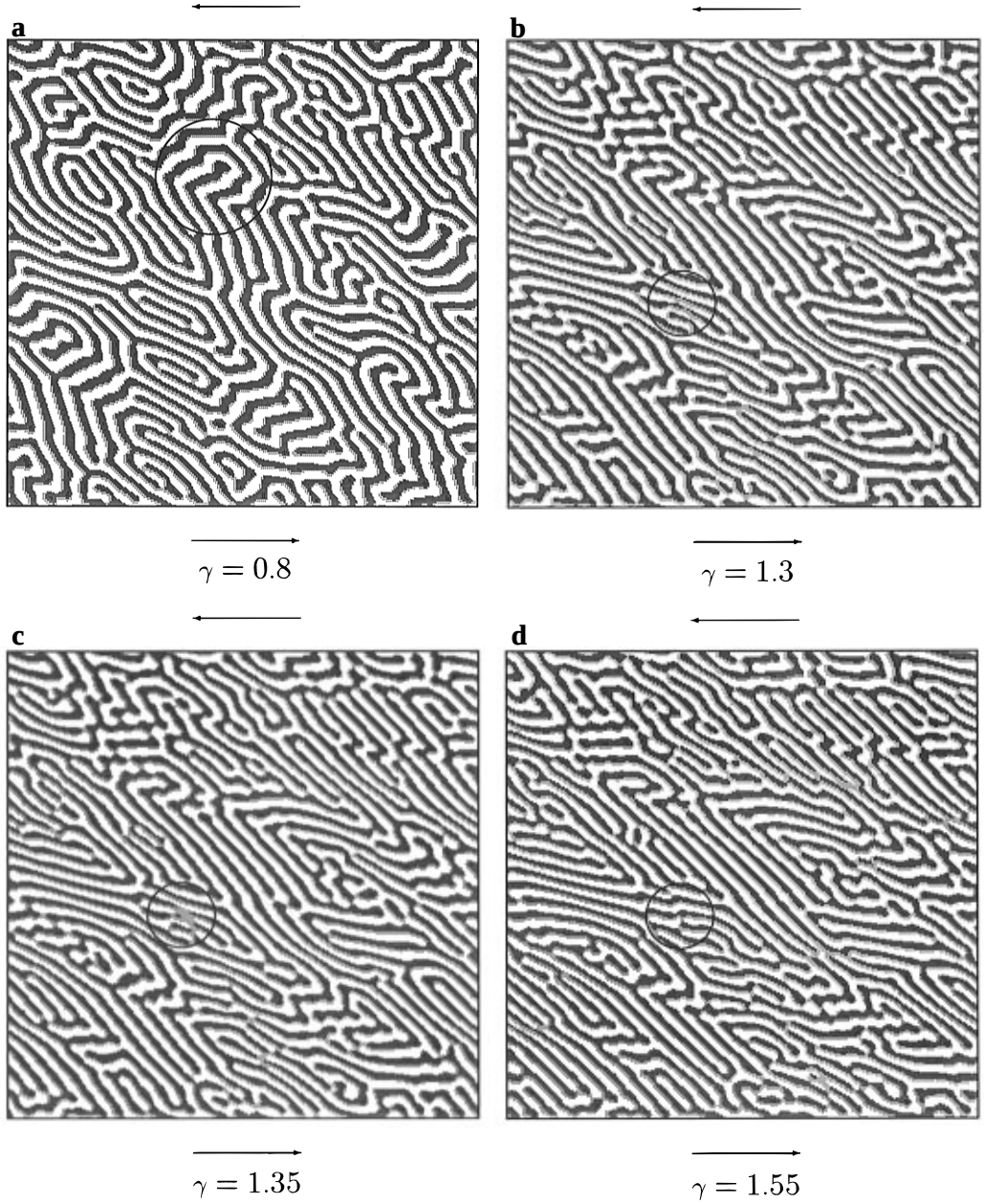

Figure 3. Density profile of the lamellar structure obtained by the simulation with $\dot{\gamma} = 10^{-3}$. The profile indicated in Figure 2 is used as the initial state, and profiles a−d show the state for shear strains γ = (a) 0.8, (b) 1.3, (c) 1.35, and (d) 1.55. Arrows show the direction of the flow.

where $I(\mathbf{n},t)$ is the discrete thermodynamic force corresponding to $\delta H_S/\delta\psi$:

$$I(\mathbf{n},t) = -A \tanh \psi(\mathbf{n},t) + \psi(\mathbf{n},t) - \tilde{D}[\langle\langle\psi(\mathbf{n},t)\rangle\rangle - \psi(\mathbf{n},t)] \quad (3.5)$$

In the present simulation, we fixed the parameters as $A = 1.26$, $\tilde{D} = 0.5$, and $\tilde{\alpha} = 0.012$ and used the sheared periodic boundary condition. This set of parameter gives the most unstable wavenumber k_e (see eq 4.12) as

$$k_e = 0.39 \quad (3.6)$$

and its growth rate Λ as

$$\Lambda = -k_e^2(\tilde{D}k_e^2 + F'(\psi{=}0)) - \tilde{\alpha} = 0.016 \quad (3.7)$$

3.2. Instability for Randomly Oriented Lamellae in Shear. From now on, we shall drop the tildes from $\tilde{D}$, $\tilde{\dot{\gamma}}$, and $\tilde{\alpha}$ and use D, $\dot{\gamma}$, and α instead. The simulation was done in the following way. First, we constructed a randomly oriented lamellar pattern by letting a rather large system ($L = 256$) relax below the order−disorder transition temperature: we set 256 × 256 small random numbers fluctuating around 0 to $\psi(\mathbf{n},t{=}0)$ and then iterated eq 3.4 with $\dot{\gamma} = 0$ for 10^5 time steps. This generates the randomly oriented lamellar pattern shown in Figure 2. Next, we applied a weak steady shear flow; i.e., we iterated eq 3.4 for $\dot{\gamma} = 10^{-3}$. We did not change the shear rate since the structural change described below is mainly determined by the shear strain rather than shear rate.

Figure 3 shows the density profiles of $\psi(\mathbf{n},t)$ for various strains. Various characteristic structural changes can be observed in these figures. In the case of (a), an undulation of lamellae can be observed in the region surrounded by the circle. On the other hand, in the cases of (b), (c), and (d), the breakup and recombination

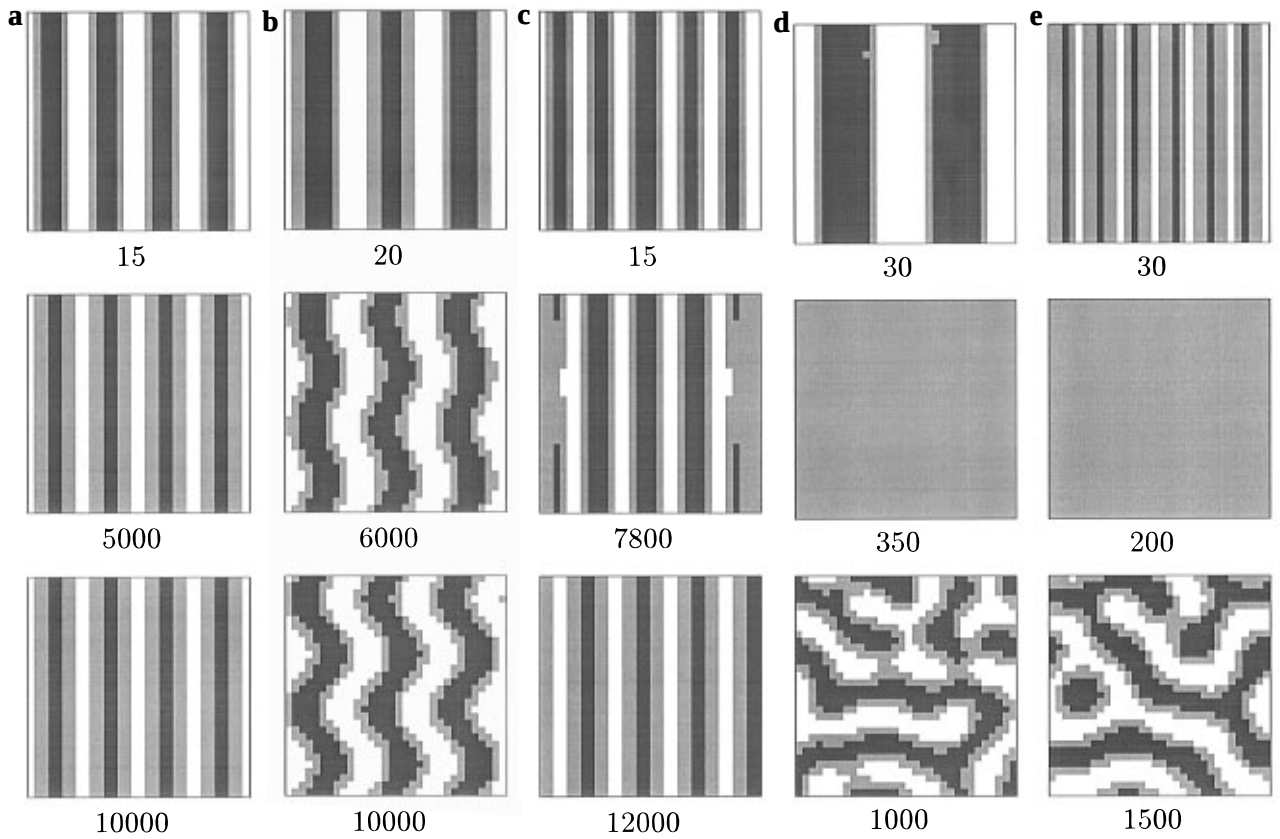

Figure 4. Relaxation of uniform lamellae of the size $L \times L = 32 \times 32$ with initial wavenumber $k =$ (a) $4/L$, (b) $3/L$, (c) $5/L$, (d) $2/L$, and (e) $6/L$. The numbers denote the time steps.

of lamellae are seen: The encircled region in (b) becomes almost disordered in (c) and again recovers the ordered state by the recombination of the broken lamellae in (d).

Note that the lamellar thickness increases in the encircled region of (a), while it decreases in the region of (b). Therefore, these two kinds of instabilities can be considered to be caused by the change of the thickness of lamellae due to the shear strain. This motivated us to investigate the stability of a lamellar structure which does not have an optimum (or equilibrium) periodicity.

3.3. Instability of Perfectly Oriented Lamellae in Compression and Expansion. To study the stability of the compressed or expanded lamellae, we conducted the following simulation. We start from the initial condition $\psi(\mathbf{n}) = A \cos(2\pi k n_x) +$ noise term and solve eq 3.4 for $\dot{\gamma} = 0$ numerically. If the initial periodicity $1/k$ is close to the optimum periodicity, the lamellae retain the initial periodicity. On the other hand, if the initial periodicity is too far from the optimum value, the lamellar structure becomes unstable. By varying the initial periodicity, we can check the stability of the lamellae with nonoptimum periodicity.

The initial condition has two parameters A and k, but it was found that the results are almost independent of the initial amplitude A. This is because the amplitude is first optimized in a rather short time (10−30 steps), and thereafter the relaxation of the periodicity takes place slowly.

Because of the periodic boundary condition, the wave vectors can take only discrete values of $k = n/L$, where n is an integer. In the present simulation, we fixed the system size at $L = 32$ and prepare five different uniform lamellae with the wave vectors $k = 2/L$, $3/L$, $4/L$, $5/L$, and $6/L$.

Figure 4 shows the time evolution of $\psi(\mathbf{n},t)$ during the relaxation processes for various initial values of k. For $k = 4/L$ (Figure 4a), the lamellae remain uniform and no structural changes are observed. The system is in the stable regime in this case. In contrast, significant structural change is observed for $k = 3/L$ (Figure 4b) and $5/L$ (Figure 4c). In the former case, which corresponds to an increase of the lamellar thickness, the lamellae start to undulate and take a corrugational shape in the end (Figure 4b). On the other hand, in the latter case, which corresponds to a decrease of lamellar thickness, the lamellar spacing begins to be modulated, and finally one of the layers merges with its neighbor (Figure 4c).

In the case of the strong deformations of $k = 2/L$ and $6/L$, the lamellar structure disappears temporarily and thereafter the normal phase ordering process starts (Figure 4d,e). Thus we observed four types of structural evolution for the lamellae which have nonoptimum periodicity: the lamellae (1) remain uniform, (2) undulate, (3) merge with the neighboring ones, and (4) melt temporarily into the disordered state, respectively. In order to know the boundaries between these regions, or the thresholds of the instabilities, we conducted a stability analysis for the expanded or compressed lamellae.

4. Stability Analysis

4.1. Equation for Complex Amplitude. We consider the vicinity of the order−disorder transition and study the free energy of a slightly modulated lamellar structure whose profile is described by

$$\psi(\mathbf{r}) = \frac{1}{2}\{A(\mathbf{r}) \exp(ikx) + \text{c.c.}\} \qquad (4.1)$$

where $A(\mathbf{r})$ represents the modulation of the uniform lamellar profile $\psi_0 = A_0 \cos kx$. We assume that $A(\mathbf{r})$ varies very slowly in space compared with the basic sinusoidal pattern. Notice that $A(\mathbf{r})$ takes complex values; the real part of A represents the modulation of the amplitude, and the imaginary part represents the phase shift.

We substitute the function (4.1) into the free energy functional (2.2) and drop the terms with nonzero Fourier components; i.e., we set

$$\int \mathrm{d}\mathbf{r}\ \partial_\alpha A(\mathbf{r})^m \exp(inkx) \simeq 0 \tag{4.2}$$

for $n \neq 0$. This approximation gives, for example, the first term in eq 2.3 as

$$\frac{a}{2}\int \mathrm{d}\mathbf{4}\ \psi^2 = \frac{a}{8}\int \mathrm{d}\mathbf{r}\ (A^2 \exp(2ikx) + \text{c.c.} + 2|A|^2) = \frac{a}{4}\int \mathrm{d}\mathbf{r}\ |A(\mathbf{r})|^2 \tag{4.3}$$

Other terms of short-range part are obtained in the similar way. On the other hand, the long-range part in the free energy (2.2) is rewritten as

$$H_\mathrm{L}\{\psi\} = \frac{1}{2}\alpha\int \mathrm{d}\mathbf{q}\ \frac{1}{q^2}\psi_{\mathbf{q}}\psi_{-\mathbf{q}} \tag{4.4}$$

where $\psi_{\mathbf{q}}(t)$ is the Fourier transform of $\psi(\mathbf{r},t)$,

$$\psi_{\mathbf{q}}(t) = \int \mathrm{d}\mathbf{r}\ \psi(\mathbf{r},t) \exp(-i\mathbf{q}\cdot\mathbf{r}) \tag{4.5}$$

Since the Fourier transform of eq 4.1 gives

$$\psi_{\mathbf{q}} = \frac{1}{2}(A_{\mathbf{q}-\mathbf{k}} + (A_{-\mathbf{q}-\mathbf{k}})^*) \tag{4.6}$$

eq 4.4 becomes

$$H_\mathrm{L}\{\psi\} = \frac{1}{8}\alpha\int \frac{\mathrm{d}\mathbf{q}}{(2\pi)^d}\frac{1}{q^2}(A_{-\mathbf{q}-\mathbf{k}}A_{\mathbf{q}-\mathbf{k}} + \text{c.c.} + 2|A_{-\mathbf{q}-\mathbf{k}}|^2) \tag{4.7}$$

where $\mathbf{k} \equiv k\hat{x}$ ($\hat{x}$ is the unit vector parallel to the x axis), and d is the spatial dimension ($d = 2$ in the present case). After some calculation, we get the following expression for the free energy:

$$H \equiv H_\mathrm{S} + H_\mathrm{L} = \int \mathrm{d}\mathbf{r}\ \left\{\frac{a}{4}|A|^2 + \frac{3}{32}g|A|^4 + \frac{D}{4}(|(ik + \partial_x)A|^2 + |\partial_y A|^2)\right\} + \frac{1}{8}\alpha\int \frac{\mathrm{d}\mathbf{q}}{(2\pi)^d}\frac{1}{q^2}(A_{-\mathbf{q}-\mathbf{k}}A_{\mathbf{q}-\mathbf{k}} + \text{c.c.} + 2|A_{-\mathbf{q}-\mathbf{k}}|^2) \tag{4.8}$$

4.2. Uniform Solution. We now seek the uniform periodic structure which minimizes eq 4.8 for a given value of k. If $A(\mathbf{r}) = A_0$ (=real constant), eq 4.8 reduces to

$$H = V\left(\frac{1}{4}f(k,a){A_0}^2 + \frac{3}{32}g{A_0}^4\right) \tag{4.9}$$

with

$$f(k,a) \equiv a + Dk^2 + \frac{\alpha}{k^2} \tag{4.10}$$

where V is the total volume of the system. If $f(k,a) > 0$, the free energy becomes minimum at $A_0 = 0$. When the initial density profile has this wave vector, its amplitude will decrease toward zero. On the other hand, if $f(k,a) < 0$, the free energy becomes minimum at

$$A_0 = \left(\frac{4}{3g}\left|f(k,a)\right|\right)^{1/2} \tag{4.11}$$

When the initial density profile has this wave vector, its amplitude will approach to this value.

It should be mentioned that after substituting eq 4.11 into eq 4.9, we can further minimize the free energy eq 4.9 with respect to k. This leads to

$$k = k_\mathrm{e} \equiv \left(\frac{\alpha}{D}\right)^{1/4} \tag{4.12}$$

which corresponds to the optimum wave vector of the lamellar phase. Furthermore, the value of a satisfying $f(k_\mathrm{e},a) = 0$ is given by

$$a = a_c \equiv -2(\alpha D)^{1/2} \tag{4.13}$$

This corresponds to the order−disorder transition temperature of the block copolymer. The lamella is the most stable if $k = k_\mathrm{e}$ and $A(\mathbf{r}) = A_0$.

4.3. Stability Analysis of Uniform Lamellar Structure. Our objective here is to study the stability of the uniform lamellar structure when it is compressed or expanded. Therefore we ask whether the lamellar structure with a given nonoptimum k value is locally stable or not. The above analysis indicates that the structure is unstable if $f(k,a) > 0$. This does not mean that the uniform lamellar structure is stable if $f(k,a) < 0$, since the structure can be unstable for small modulation of the structure.

To check the stability of the uniform lamella in the region of $f(k,a) < 0$, we consider the perturbation

$$A(\mathbf{r}) = A_0 + \epsilon(\mathbf{r}) \tag{4.14}$$

Since $A(\mathbf{r})$ is complex, $\epsilon(\mathbf{r})$ is generally written as

$$\epsilon(\mathbf{r}) = u(\mathbf{r}) + iv(\mathbf{r}) \tag{4.15}$$

with real functions $u(\mathbf{r})$ and $v(\mathbf{r})$. Substituting eq 4.14 as well as its Fourier component

$$A_{\mathbf{q}} = A_0\delta(\mathbf{q}) + \epsilon_{\mathbf{q}} \tag{4.16}$$

to the complex amplitude equation (4.8), we calculate the increment of the free energy up to the second order of ϵ. Here the approximation (4.2) is used again. For example, in the expression

$$\int \frac{\mathrm{d}\mathbf{q}}{(2\pi)^d}\frac{1}{q^2}A_{-\mathbf{q}-\mathbf{k}}A_{\mathbf{q}-\mathbf{k}} = \frac{A_0}{k^2}(A_0\delta(-2\mathbf{k}) + 2\epsilon_{-2\mathbf{k}}) + \int \frac{\mathrm{d}\mathbf{q}}{(2\pi)^d}\frac{1}{q^2}\epsilon_{-\mathbf{q}-\mathbf{k}}\epsilon_{\mathbf{q}-\mathbf{k}} \tag{4.17}$$

the first two terms on the right-hand side are neglected because of eq 4.2. As a result, we obtain the following expression for the incremental free energy $\Delta H = H\{A_0 + \epsilon\} - H\{A_0\}$:

$$\Delta H = \int d\mathbf{r} \left[-\frac{1}{2}\left(a + Dk^2 + \frac{3\alpha}{2k^2}\right)u^2 - \frac{\alpha}{4k^2}v^2 + \frac{Dk}{2}\{u(\partial_x v) - (\partial_x u)v\} + \frac{D}{4}\{(\partial_x u)^2 + (\partial_y u)^2 + (\partial_x v)^2 + (\partial_y v)^2\}\right] + \frac{1}{8}\alpha \int \frac{d\mathbf{q}}{(2\pi)^d}\frac{1}{q^2}(\epsilon_{-\mathbf{q}-\mathbf{k}}\epsilon_{\mathbf{q}-\mathbf{k}} + \text{c.c.} + 2|\epsilon_{-\mathbf{q}-\mathbf{k}}|^2) \quad (4.18)$$

To study the stability, we may assume, without loss of generality, as follows.

$$u = U_{ss} \sin w_x x \sin w_y y + U_{sc} \sin w_x x \cos w_y y + U_{cs} \cos w_x x \sin w_y y + U_{cc} \cos w_x x \cos w_y y \quad (4.19a)$$

$$v = V_{ss} \sin w_x x \sin w_y y + V_{sc} \sin w_x x \cos w_y y + V_{cs} \cos w_x x \sin w_y y + V_{cc} \cos w_x x \cos w_y y \quad (4.19b)$$

This gives ΔH in the following form:

$$\Delta H = V[J(U_{ss},V_{cs}) + J(U_{sc},V_{cc}) + J(U_{cs},-V_{ss}) + J(U_{cc},-V_{sc})] \quad (4.20)$$

where $J(U,V)$ is an quadratic function of U and V

$$J(U,V) = \xi U^2 + 2\eta UV + \zeta V^2 \quad (4.21)$$

and the coefficients ξ, η, and ζ are given by

$$\xi = \frac{1}{16}\left\{-\left(2a + 2Dk^2 + \frac{3\alpha}{k^2}\right) + D(w_x^2 + w_y^2) + \frac{\alpha}{2}\left(\frac{1}{(k - w_x)^2 + w_y^2} + \frac{1}{(k + w_x)^2 + w_y^2}\right)\right\} \quad (4.22a)$$

$$\eta = \frac{1}{32}\left\{-4Dkw_x + \alpha\left(\frac{1}{(k - w_x)^2 + w_y^2} - \frac{1}{(k + w_x)^2 + w_y^2}\right)\right\} \quad (4.22b)$$

$$\zeta = \frac{1}{16}\left\{-\frac{\alpha}{k^2} + D(w_x^2 + w_y^2) + \frac{\alpha}{2}\left(\frac{1}{(k - w_x)^2 + w_y^2} + \frac{1}{(k + w_x)^2 + w_y^2}\right)\right\} \quad (4.22c)$$

If the quadratic form (4.21) is positive definite for all (w_x, w_y), the uniform lamellar structure is stable. On the other hand, if there are some (w_x, w_y) which make the quadratic form negative, the uniform lamellar structure is unstable against the modulation of the wave vector (w_x, w_y). Now we may assume (w_x, w_y) is not equal to (0, 0) since for $(w_x, w_y) = (0, 0)$ the analysis becomes equivalent to that done for uniform lamella. For $(w_x, w_y) \neq (0, 0)$, is easy to confirm that both ξ and ζ are positive in the region of $f(k,a) < 0$. Therefore the stability condition reduces to

$$S \equiv \xi\zeta - \eta^2 > 0 \quad (4.23)$$

Expanding S for small values of w_x and w_y, we get

$$S = g(k,a)w_x^2 + h(k,a)w_y^2 \quad (4.24)$$

where

$$g(k,a) = \frac{1}{128}\left\{-\left(D + \frac{3\alpha}{k^4}\right)\left(a + Dk^2 + \frac{\alpha}{k^2}\right) - 2\left(Dk - \frac{\alpha}{k^3}\right)^2\right\} \quad (4.25a)$$

$$h(k,a) = -\frac{1}{128}\left(D - \frac{\alpha}{k^4}\right)\left(a + Dk^2 + \frac{\alpha}{k^2}\right) \quad (4.25b)$$

Using a_c and k_e defined by eqs 4.12 and 4.13, these equations are rewritten as

$$g(k,a) = \frac{a_c}{256k_e^2k^4}\left\{a(k^4 + 3k_e^4) - \frac{a_c}{2k_e^2k^2}(3k^8 + 5k_e^8)\right\} \quad (4.26a)$$

$$h(k,a) = \frac{a_c}{256k_e^2k^4}\left\{a(k^4 - k_e^4) - \frac{a_c}{2k_e^2k^2}(k^8 - k_e^8)\right\} \quad (4.26b)$$

The stability of the uniform lamellar structure is determined by the signs of $g(k,a)$ and $h(k,a)$.

(i) If $g(k,a) > 0$ and $h(k,a) > 0$, the uniform lamellar structure is stable and retains its periodicity even if it is not the optimum one. This corresponds to the situation shown in Figure 4a. The region is designated by MS (metastable) in Figure 5.

(ii) If $g(k,a) > 0$ and $h(k,a) < 0$, the uniform lamellar structure is unstable against the modulation whose wave vector is parallel to the lamellar plane. This corresponds to the undulational instability shown in Figure 4b. This region is designated by UI(1) in Figure 5.

(iii) If $g(k,a) < 0$ and $h(k,a) > 0$, the uniform lamellar structure is unstable against the modulation whose wave vector is normal to the lamellar plane. This corresponds to the Eckhaus instability shown in Figure 4c. The region is designated by EI in Figure 5.

(iv) If $g(k,a) < 0$ and $h(k,a) < 0$, both the undulational instability and the Eckhaus instability can take place. However, we have numerically checked that the undulational mode is more unstable than the Eckhaus mode; i.e., we checked at several points (e.g., $(k/k_e, a/|a_c|) = (-1.1, 0.84)$, $(-1.16, 0.81)$, $(-1.3, 0.76)$, etc.) in this region that the following inequality holds for the same value of U_{ss}, U_{sc}, ..., V_{cc}:

$$\Delta H_{\text{undulation}} < \Delta H_{\text{Eckhaus}} \quad (4.27)$$

Therefore we classified this region into the undulational instability (UI(2) in Figure 5).

Finally, if $f(k,a) > 0$, the lamellae will melt uniformly since the free energy decreases with the decrease of the amplitude. This corresponds to the situation shown in Figure 4d,e. We call such a region the melt instability region. It is designated by MI in the $k-a$ plane in Figure 5.

5. Summary and Discussion

In this paper, we have discussed the structural changes of randomly oriented lamellae of block copooymers under shear flow. In the computer simulation, we observed two typical ways of structural change: one is breakup and recombination of the lamellae, and the other is the undulation of lamellae.

We have attributed the occurrence of these structural changes to the local deviation of the lamellar thickness

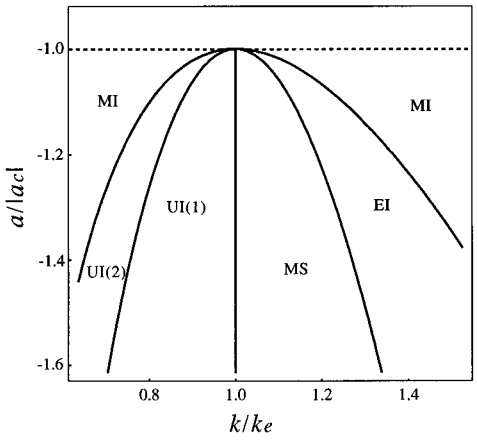

Figure 5. Stability diagram, where a is a model parameter corresponding to the temperature, and k is the wavenumber which is proportional to the inverse of the lamellar thickness. In the region designated MS, the uniform lamellar structure is metastable. In the other regions, the uniform lamellar structure is unstable, and the melting instability (MI), the Eckhaus instability (EI), or the undulational instability (UI) occurs. Here $a_c \equiv -2(\alpha D)^{1/2}$ corresponds to the order−disorder transition temperature of the system, and $k_e \equiv (\alpha/D)^{1/4}$ is the wavenumber of the stable uniform lamellae in equilibrium.

from its optimum value due to the shear flow.[11] We then investigated the stability of the uniform lamellae under the thickness variation by the simulation. The result is that the compression and expansion induce an Eckhaus type instability and an undulational type instability respectively for small variation and the melt instability for large variation. We have derived analytically the stability diagram in the temperature and inverse lamellar thickness plane by constructing the amplitude equation for the free energy. This enables us to estimate the magnitude of the deformation at which the structural change starts to occur.

The present analysis indicates that a new type of instability, the Eckhaus instability, can take place in block copolymer lamellae. This is a result of the fact that our analysis allows a more general modulation of the structure than was allowed in the earlier analyses.[11,12]

The present work, however, is concerned with the initial stage of the structural change. Further work is clearly needed to understand how the randomly oriented lamellae turn into oriented lamellae. (i) Computer simulation has to be done for large strain. We have conducted a simulation for large strains ($\gamma \lesssim 20$) and observed the formation of a perfectly aligned lamellae whose normal is parallel to the shear parallel to the shear gradient. This is, however, only for one run and the effects of shear rate and the temperature have not been studied. Also three-dimensional simulation has to be done in order to study the possibility of the other types (i.e., perpendicular and transverse) of lamellar alignment. (ii) The present analysis is a quasi-static one. Full dynamical treatment is needed to study how the shear rate affects the instability and how the structure evolves in time. Research is now being done in these directions, and the result will be published in future.

Acknowledgment. We would like to express our appreciation to Prof. T. Ohta, Dr. T. Kawakatsu, and Dr. S. Komura for informative discussions. We also thank the reviewers for giving us very helpful comments. H.K. acknowledges the support of the Ministry of Education, Science and Culture, Japan (Grant-in-Aid for Scientific Research No. 0657).

References and Notes

(1) Keller, A.; Pedemonte, E.; Willmouth, F. M. *Kolloid-Z. Z. Polym* **1970**, *238*, 385. Keller, A.; Pedemonte, E.; Willmouth, F. M. *Nature* **1970**, *225*, 538. Folkes, M. J.; Keller, A.; Scalisi, F. P. *Kolloid-Z. Z. Polym* **1973**, *251*, 1.
(2) Hadziioannou, G.; Mathis, A.; Skoulios, A. *Colloid Polym. Sci.* **1979**, *257*, 136. Hadziioannou, G.; Skoulios, A. *Macromolecules* **1982**, *15*, 258.
(3) Koppi, K. A.; Tirrell, M.; Bates, F. S.; Almdal, K.; Colby, R. H. *J. Phys. II Fr.* **1992**, *2*, 1941.
(4) Winey, K. I.; Patel, S. S.; Larson, R. G.; Watanabe, H. *Macromolecules* **1993**, *26*, 2542.
(5) Winey, K. I.; Patel, S. S.; Larson, R. G.; Watanabe, H. *Macromolecules* **1993**, *26*, 4373.
(6) Okamoto, S.; Saijo, K.; Hashimoto, T. *Macromolecules* **1994**, *27*, 5547.
(7) Zhang, Y.; Wiesner, U.; Spiess, H. W. *Macromolecules* **1995**, *28*, 778.
(8) Patel, S. S.; Larson, R. G.; Winey, K. I.; Watanabe, H. *Macromolecules* **1995**, *28*, 4313.
(9) Gupta, V. K.; Krishnamoorti, R.; Kornfield, J. A. *Macromolecules* **1995**, *28*, 4464.
(10) Zhang, Y.; Wiesner, U. *J. Chem. Phys.* **1995**, *103*, 4784.
(11) Amundson, K.; Helfand, E. *Macromolecules* **1993**, *26*, 1324.
(12) Wang, Z.-G. *J. Chem. Phys.* **1994**, *100*, 2298.
(13) Williams, D. R. M.; MacKintosh, F. C. *Macromolecules* **1994**, *27*, 7677.
(14) Fredrickson, G. H. *J. Rheol.* **1994**, *38*, 1045.
(15) Goulian, M.; Milner, S. T. *Phys. Rev. Lett.* **1995**, *74*, 1775.
(16) Ohta, T.; Kawasaki, K. *Macromolecules* **1986**, *19*, 2621.
(17) Oono, Y.; Shiwa, Y. *Mod. Phys. Lett. B* **1987**, *1*, 49.
(18) Oono, Y.; Puri, S. *Phys. Rev. A* **1988**, *38*, 434. Puri, S.; Oono, Y. *Phys. Rev. A* **1988**, *38*, 1542.
(19) Bahiana, M.; Oono, Y. *Phys. Rev. A* **1990**, *41*, 6763.
(20) Manneville, P. *Dissipative Structures and Weak Turbulence*; Academic Press: New York, 1990.
(21) Ohta, T.; Enomoto, Y.; Harden, J. L.; Doi, M. *Macromolecules* **1993**, *26*, 4928.

MA9512216